Theoretical Study of the Electronic Structure of Group 6 $[M(CO)_5X]^-$ Species (X = NH_2, OH, Halide, H, CH_3) and a Reinvestigation of the Role of π-Donation in CO Lability

Stuart A. Macgregor* and David MacQueen

Department of Chemistry, Heriot-Watt University, Riccarton, Edinburgh EH14 4AS, U.K.

Received March 31, 1999

Density functional calculations have been employed to investigate the electronic structure of $[M(CO)_5X]^-$ species (M = Cr, Mo, W; X = NH_2, OH, halide, H, CH_3) and to compute CO ligand dissociation energies. The calculations indicate that CO loss is most facile from the cis position, and CO dissociation energies are computed to increase along the series X = NH_2 < OH < F < Cl < Br < I < CH_3 < H. These results are in agreement with available experimental data. Trends in CO dissociation are related to the ability of X to stabilize the unsaturated 16e $[M(CO)_4X]^-$ species formed. In addition, π-destabilization of the ground-state $[M(CO)_5X]^-$ species is equally significant. Analysis of the electronic structure of the 18e species shows that Xπ−dπ 4e destabilization results in hybridization at the metal center which enhances trans M−CO but reduces cis M−CO π-back-donation. Strong π-donation from X also induces σ-antibonding interactions between the metal and the cis CO ligands. A fragment analysis reveals that these effects are strongest for the "hard" fluoride, hydroxide, and amide ligands.

Introduction

Recently, there has been considerable interest in the chemistry of low-valent transition metal systems which combine "soft" metal centers with "hard" donor ligands. Such species might be thought to be intrinsically unstable due to the apparent "soft−hard" mismatch. However, an increasing number of examples of low-valent transition metal fluorides,[1] alkoxides,[2] and amides[3] have been characterized experimentally and progress has been made in developing systematic routes to the synthesis of such species.[4] As well as the intrinsic interest in the study of the metal−ligand mismatch, there is interest in low-valent metal alkoxides and amides because of their role as potential intermediates in catalytic cycles.[5]

We are interested in using theoretical methods to understand the electronic structure of low-valent transition metal systems featuring "hard" donor ligands and the consequences that this combination has for the reactivity of such species. One interesting series of complexes are the anionic substituted pentacarbonyl species of the form $[M(CO)_5X]^-$, where M = Cr, Mo, or W and X is a π-donor. These species all exhibit enhanced CO lability compared to that of the hexacarbonyl parent, but this effect is especially pronounced when X = F or OH. In this work, we aim to model the CO dissociation process using density functional calculations and to investigate the role of X in determining the ease of CO loss through studying the underlying electronic structure of these species.

Anionic chloro, bromo, and iodo $[M(CO)_5X]^-$ species have been known for some time and readily undergo CO substitution reactions.[6] Kinetic studies[7] suggest that this process occurs via a dissociative mechanism and that the rate of reaction is a function of both the halide (X = Cl > Br > I) and the metal center (M = Mo > Cr > W). CO dissociation from $[M(CO)_5Cl]^-$ is approximately 10^7-10^9 times faster than that from the equivalent $M(CO)_6$ complex.[8] In contrast, far less information is available on the anionic fluoro analogues. IR spectroscopic data for $[M(CO)_5F]^-$ species were reported in the 1970s,[9] but recent studies by Darensbourg and co-workers suggest that $[W(CO)_5F]^-$, at least, is only stable under an atmosphere of CO.[10] Removal of CO results in the reversible formation of a triply bridged fluoride dimer:

$$2[W(CO)_5F]^- + F^- \underset{+CO}{\overset{-CO}{\rightleftharpoons}} [W_2(CO)_6F_3]^{3-}$$

Analogous $[M(CO)_5OH]^-$ species also lose CO in a similar fashion and have been reported to form either dimers (M = Mo, W)[11] or tetramers (M = Cr, Mo, W).[12] $[W(CO)_5OR]^-$ species (R = H,[13] CH_3[14]) have been characterized in solution

(1) (a) Doherty, N. M.; Hoffman, N. W. *Chem. Rev.* **1991**, *91*, 553. (b) Clark, H. C. S.; Fawcett, J.; Holloway, J. H.; Hope, E. G.; Peck, L. A.; Russell, D. R. *J. Chem. Soc., Dalton Trans.* **1998**, 1249. (c) Pilon, M. C.; Grushin, V. V. *Organometallics* **1998**, *17*, 1774. (d) Cronin, L.; Higgitt, C. L.; Karch, R.; Perutz, R. N. *Organometallics* **1997**, *16*, 4920.

(2) (a) Bryndza, H. E.; Tam, W. *Chem. Rev.* **1988**, *88*, 1163. (b) Grushin, V. V.; Alper, H. *Organometallics* **1996**, *15*, 5242. (c) Mann, G.; Hartwig, J. F. *J. Am. Chem. Soc.* **1996**, *118*, 13109. (d) Kaplan, A. W.; Bergman, R. G. *Organometallics* **1997**, *16*, 1106. (e) Widenhoefer, R. A.; Zhong, H. A.; Buchwald, S. L. *J. Am. Chem. Soc.* **1997**, *119*, 6787. (f) Bennett, M. A.; Jin, H.; Li, S.; Rendina, L. M.; Willis, A. C. *J. Am. Chem. Soc.* **1995**, *117*, 8335.

(3) (a) Fryzuk, M. D.; Montgomery, C. D. *Coord. Chem. Rev.* **1989**, *95*, 1. (b) Hartwig, J. F. *J. Am. Chem. Soc.* **1996**, *118*, 7010. (c) Bryndza, H. E.; Fultz, W. C.; Tam, W. *Organometallics* **1985**, *4*, 939.

(4) (a) Ritter, J. C. M.; Bergman, R. G. *J. Am. Chem. Soc.* **1998**, *120*, 6826. (b) Kaplan, A. W.; Ritter, J. C. M.; Bergman, R. G. *J. Am. Chem. Soc.* **1998**, *120*, 6828.

(5) (a) Beller, M.; Eichberger, M.; Trauthwein, H. *Angew. Chem., Int. Ed. Engl.* **1997**, *36*, 2225. (b) Casalnuovo, A. L.; Calabrese, J. C.; Milstein, D. *J. Am. Chem. Soc.* **1988**, *110*, 6738.

(6) Abel, E. W.; Butler, I. S.; Reid, J. G. *J. Chem. Soc.* **1963**, 2068.

(7) Allen, A. D.; Barrett, P. F. *Can. J. Chem.* **1968**, *46*, 1655.

(8) (a) Graham, J. R.; Angelici, R. J. *Inorg. Chem.* **1967**, *6*, 2082. (b) Darensbourg, D. J. *Adv. Organomet. Chem.* **1982**, *21*, 113.

(9) Douglas, W.; Ruff, J. K. *J. Organomet. Chem.* **1974**, *65*, 65.

(10) Darensbourg, D. J.; Klausmeyer, K. K.; Reibenspies, J. H. *Inorg. Chem.* **1995**, *34*, 4933.

(11) (a) Hieber, V. W.; Englert, K.; Rieger, K. *Z. Anorg. Allg. Chem.* **1959**, *300*, 304. (b) Hieber, V. W.; Englert, K.; Rieger, K. *Z. Anorg. Allg. Chem.* **1959**, *300*, 295.

(12) (a) McNeese, T. J.; Mueller, T. E.; Wierda, D. A.; Darensbourg, D. J.; Delord, T. J. *Inorg. Chem.* **1985**, *24*, 3465. (b) Lin, J. T.; Yeh, S. K.; Lee, G. H.; Wang, Y. *J. Organomet. Chem.* **1989**, *361*, 89.

10.1021/ic990355n CCC: $18.00
Published on Web 10/18/1999

by IR spectroscopy, and a crystal structure of $[W(CO)_5OPh]^-$ has been published.[15] The rate constant for CO loss from $[W(CO)_5OPh]^-$ has been determined to be 2.15×10^{-2} s^{-1} at 5 °C compared to 1.01×10^{-4} s^{-1} for $[W(CO)_5Cl]^-$ under similar conditions.[16] To our knowledge, no analogous amido pentacarbonyl species has been reported, although work from Darensbourg's group has shown that deprotonation of $M(CO)_4(O_2CCH_2NHR)$ (M = Cr, W; R = H, CH_3) produces a transient amido tetracarbonyl species which exhibits high CO lability.[17] Analogous behavior has been observed with other chelating amine ligands.[18] The nature of X therefore plays a crucial role in CO dissociation which is most facile for fluoride or O- (and probably N-) based π-donor ligands. The importance of π-donation is emphasized by the fact that $[M(CO)_5H]^-$ and $[M(CO)_5CH_3]^-$ analogues do not readily undergo CO substitution reactions.[19]

Similar behavior has been reported for the neutral isoelectronic $M(CO)_5X$ analogues (M = Mn, Re; X = Cl, Br, I). CO dissociation exhibits the same halide dependency and is approximately 10^5-10^6 times faster than that for dimeric $M_2(CO)_{10}$.[20,21] The parent $[M(CO)_6]^+$ species and $Re(CO)_5H$ are substitution-inert, although $Mn(CO)_5H$ is thought to react via either a hydride migration or radical chain process.[22] There are various reports of the preparation of $Re(CO)_5F$ in the literature, but the precise nature of the product formed depends on the reaction conditions employed.[1a] The difficulty in isolating $Re(CO)_5F$ may reflect the strong labilizing effect of the fluoride ligand: It is known that the related $ReF(CO)_3(PPh_3)_2$ complex exhibits enhanced CO lability compared to that of its chloro analogue.[23] Neither $Mn(CO)_5F$ nor any neutral alkoxo− or amido−pentacarbonyl complex of manganese or rhenium has been reported.

Determining the site of CO loss has been a particular focus of the work carried out on these neutral $M(CO)_5X$ species. Atwood and Brown demonstrated that, for $Mn(CO)_5Br$, the 16e intermediate formed upon CO loss is fluxional and that the rate of CO dissociation from a site cis to Br is at least 10 times that of the trans CO ligand.[24] Theoretical methods have also been employed to address the site preference issue.[25,26] In principle, X could influence CO labilization by affecting the energy of the ground-state 18e $M(CO)_5X$ species, the 16e $M(CO)_4X$ species formed upon CO loss, or both. Ground-state effects have been assessed by comparing bond distances and vibrational frequencies or by calculating the energy required to remove a CO ligand to form two alternative T_{CO} and T_X complex fragments (see Scheme 1). In this approach, the geometries of these species are unchanged from those found within the 18e species, and it was initially suggested that these complex fragments would resemble transition states for the CO dissociation process. The role of X in stabilizing the 16e intermediate has been quantified by calculating the relaxation energy when the T_{CO} and T_X complex fragments are allowed to optimize.

Scheme 1

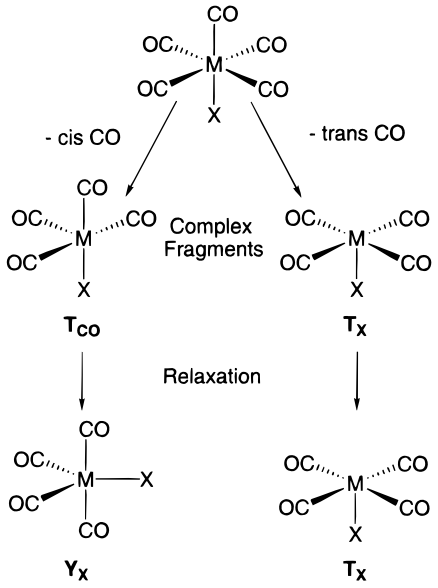

Atwood and Brown proposed a site preference model whereby the labilizing effect of X reflects its ability to stabilize the complex fragment produced. For a square-pyramidal geometry, ligands which are weak σ-donors and poor π-acceptors will preferentially occupy a basal site over CO.[20] Using Fenske−Hall calculations, Lichtenberger and Brown confirmed that square-pyramidal $Mn(CO)_4Br$ was more stable as the T_{CO} form.[25] However, this approach failed to account for the greater cis lability in $Mn(CO)_5Br$ compared to $[Mn(CO)_6]^+$, as the energies calculated to remove CO to produce a T_{CO} complex fragment were comparable in both cases. These authors emphasized the importance of relaxation effects in the $Mn(CO)_4Br$ complex and showed that a π-donor would stabilize a Y_X distorted trigonal-pyramidal geometry. This structure is favored as the C_{2v} $\{M(CO)_4\}$ fragment has two low-lying vacant orbitals which can accept both σ- and π-electron density from X (**1** and **2**). This explanation is also consistent with the inertness

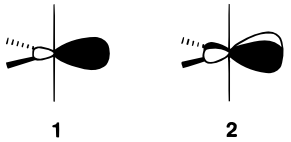

of $Re(CO)_5H$ toward CO substitution where π-stabilization of any intermediate formed would not be possible. Relaxation effects were found to be less important for the T_X complex fragment.

(13) Darensbourg, D. J.; Meckfessel Jones, M. L.; Reibenspies, J. H. *Inorg. Chem.* **1996**, *35*, 4406.
(14) Darensbourg, D. J.; Gray, R. L.; Ovalles, C.; Pala, M. *J. Mol. Catal.* **1985**, *29*, 285.
(15) Darensbourg, D. J.; Sanchez, K. M.; Reibenspies, J. H.; Rheingold, A. L. *J. Am. Chem. Soc.* **1989**, *111*, 7094.
(16) Darensbourg, D. J.; Klausmeyer, K. K.; Draper, J. D.; Chojnacki, J. A.; Reibenspies, J. H. *Inorg. Chim. Acta* **1998**, *270*, 405.
(17) Darensbourg, D. J.; Draper, J. D.; Reibenspies, J. H. *Inorg. Chem.* **1997**, *36*, 3648.
(18) (a) Darensbourg, D. J.; Klausmeyer, K. K.; Reibenspies, J. H. *Inorg. Chem.* **1996**, *35*, 1535. (b) Darensbourg, D. J.; Draper, J. D.; Larkins, D. L.; Frost, B. J.; Reibenspies, J. H. *Inorg. Chem.* **1998**, *37*, 2538.
(19) (a) Darensbourg, D. J.; Hanckel, R. K.; Bauch, C. G.; Pala, M.; Simmons, D.; White, J. N. *J. Am. Chem. Soc.* **1985**, *107*, 7463. (b) Woodward, S. In *Comprehensive Organometallic Chemistry*; Abel, E. W., Stone, F. G. A., Wilkinson, G., Eds.; Pergamon Press: Oxford, U.K., 1996; Vol. 5, p 223.
(20) Atwood, J. D.; Brown, T. L. *J. Am. Chem. Soc.* **1976**, *98*, 3160 and references therein.
(21) Wawersik, H.; Basolo, F. *Inorg. Chim. Acta* **1969**, *3*, 113.
(22) (a) Byers, B. H.; Brown, T. L. *J. Am. Chem. Soc.* **1975**, *97*, 947. (b) Berry, A.; Brown, T. L. *J. Organomet. Chem.* **1971**, *33* C67.
(23) Hoffman, N. W.; Prokopuk, N.; Robbins, M. J.; Jones, C. M.; Doherty, N. M. *Inorg. Chem.* **1991**, *30*, 4177. $MnF(CO)_3(PPh_3)_2$ has also been synthesized: Drew, D.; Darensbourg, D. J.; Darensbourg, M. Y. *Inorg. Chem.* **1975**, *14*, 1579. A series of Re alkoxides and aryloxides of the form $Re(CO)_3L_2OR$, where L = phosphine and arsine ligands, have been characterized: Simpson, R. D.; Bergman, R. G. *Organometallics* **1993**, *12*, 781.
(24) Atwood, J. D.; Brown, T. L. *J. Am. Chem. Soc.* **1975**, *97*, 3380.
(25) Lichtenberger, D. L.; Brown, T. L. *J. Am. Chem. Soc.* **1978**, *100*, 366.
(26) Davy, R. D.; Hall, M. B. *Inorg. Chem.* **1989**, *28*, 3524.

On the face of it, arguments based on π-bonding in the 18e $M(CO)_5X$ species can also provide a simple rationale for the greater lability of the cis CO ligands. In C_{4v} symmetry, the trans CO can engage in two stabilizing interactions with the M−X π-system. Only one such interaction is possible for the cis CO ligands, resulting in a weaker M−C bond. Support for this argument comes from crystallographic data on group 6 and 7 substituted pentacarbonyl species where, for a given molecule, trans M−C distances are consistently shorter than cis M−C distances. However, over a series of related compounds trends in M−C distances do not reflect variations in CO lability.[20] In addition, as pointed out by Lichtenberger and Brown, π-bonding arguments fail to account for the greater cis lability in $Mn(CO)_5Br$ compared to $[Mn(CO)_6]^+$. Competition for π-back-donation in the latter should be more intense, yet this species is substitution-inert. Attempts by these authors to relate CO dissociation to trends in CO fragment Mulliken orbital populations or M−CO overlap populations also proved either inconclusive or inconsistent with experimental observation.[25]

In a later study, Davy and Hall performed RHF calculations on $Mn(CO)_5X$ species (X = H, Cl).[26] They concluded that both ground-state and relaxation effects favored cis CO loss although their relative importance depended on X. For X = H, both effects were comparable in magnitude. When X = Cl, relaxation effects were more significant due to the π-donor capacity of Cl, although a distorted T_{CO} rather than a Y_X structure was found for $Mn(CO)_4Cl$. No comparison with the parent $[Mn(CO)_6]^+$ complex was made. More recently, in a study of the photolytic processes of $Mn(CO)_5Cl$ using density functional theory, Baerends and co-workers found a Y_X geometry to be the most stable form for $Mn(CO)_4Cl$.[27]

In this study, we shall use density functional methods to investigate CO dissociation from group 6 $[M(CO)_5X]^-$ species. X will be a variety of π-donors (NH_2, OH, halides) and σ-donors (H, CH_3). We shall also extend our study to include the neutral $M(CO)_6$ and $M'(CO)_5X$ species (M′ = Mn, Re). As we have a wider interest in the interaction between "hard" ligands and "soft", low-valent metal centers, which generally do not have vacant orbitals to accept π-electron density from X, we are particularly concerned with the effect that X has on the electronic structure of the 18e $[M(CO)_5X]^-$ species. This will allow us to readdress the issue of ground-state effects in promoting cis CO lability.

Computational Details

All calculations used the Amsterdam Density Functional program (ADF, version 2.3.1) developed by Baerends et al.[28] and employed the numerical integration scheme of te Velde and Baerends.[28c] A triple-ζ−STO basis set was employed for all metal atoms while all other atoms were described using a double-ζ−STO basis set extended by a polarization function. An auxiliary set of s, p, d, f, and g STO basis functions centered on all nuclei was used to fit the molecular density and describe accurately the Coulomb and exchange potentials in each SCF cycle.[29] Core electrons (the 1s electrons for C, N, O, and F and up to and including 2p for Cr, Mn and Cl, 3d for Mo and Br, and 4d for I, W, and Re) were treated using the frozen-core approximation. Geometry optimization was carried out using the local density approximation (LDA) employing the parametrization of Vosko, Wilk, and Nusair[30] and used the optimization procedure developed by Versluis and Ziegler.[31] The quasi-relativistic corrections of Ziegler and co-workers were also included.[32] Energies of all optimized structures were then recalculated with the nonlocal (NL) corrections of Becke[33] (exchange) and Perdew[34] (correlation) included. All molecules were initially optimized with the highest possible symmetry, and the stationary points located were characterized by frequency analyses. In some instances, low-energy imaginary frequencies were computed. This point was investigated further for $[W(CO)_5Br]^-$, and it was found that the true minimum exhibits a slight C_{2v} distortion. However, the energy of this species did not differ significantly from that of the C_{4v} geometry, and because of the large number of species in this study, the higher symmetry results will be used. Optimized Cartesian coordinates for all structures are supplied as Supporting Information. For ease of analysis, the structures of $[M(CO)_5OH]^-$, $[M(CO)_5NH_2]^-$, and $[M(CO)_5CH_3]^-$ were calculated with the plane of symmetry containing two cis CO ligands. In all cases, the alternative structure with the plane of symmetry bisecting the $C_{cis}-M-C_{cis}$ angle was close in energy (within 1 kcal/mol). Orbital diagrams were produced with MOLDEN[35] after interfacing with ADFrom.[36]

Results

1. Optimized Geometries for $[M(CO)_5X]^-$ Species. Calculated structural parameters for $[W(CO)_5X]^-$ are presented in Table 1, along with any available experimental data for comparison. Similar trends are seen in the optimized structures for the Cr and Mo analogues. Figure 1 displays the optimized structure of $[W(CO)_5NH_2]^-$, as well as the labeling scheme adopted. Calculated geometries all exhibit C_{4v} or pseudo-C_{4v} symmetry at the metal center. For X = CH_3, NH_2, or OH (formally C_s symmetry), average values for the in-plane $W-C_{cis}$, $C-O_{cis}$, and $X-W-C_{cis}$ parameters are given in Table 1. The amido ligands in $[M(CO)_5NH_2]^-$ species all exhibit a pyramidal geometry, indicative of little forward donation of π-electron density to the metal center.[3a,37]

The data in Table 1 show reasonable agreement between computed and experimental geometries. In all cases, the $W-C_{trans}$ distance is shorter than the $W-C_{cis}$ distance and the corresponding $C-O_{trans}$ distance is longer than $C-O_{cis}$. This is also found experimentally and is consistent with enhanced π-back-donation in the $W-CO_{trans}$ bond. The difficulty in relating experimental W−C distances to trends in CO lability can also be seen in our calculations. Computed $W-C_{cis}$ and $W-C_{trans}$ distances vary little as a function of X, and calculated M−C distances are always shorter in $[W(CO)_5X]^-$ species compared to the corresponding (less labile) $W(CO)_6$ parent (W−C = 2.025 Å and C−O = 1.147 Å, using the same method).

2. Electronic Structure of $[M(CO)_5X]^-$ Species. For each $[M(CO)_5X]^-$ series, trends in electronic structure were similar as the nature of X varied, and we shall focus attention here on the case where M = W. $[W(CO)_5H]^-$ exhibits many features common to all these species. In C_{4v} symmetry, the metal-based t_{2g} orbitals are split to give the 10e HOMO and $3b_2$ orbital. To lower energy, the $11a_1$ orbital is predominantly W−H σ-bonding, and there follows a series of CO-based orbitals arising from

(27) Wilms, M. P.; Baerends, E. J.; Rosa, A.; Stufkens, D. J. *Inorg. Chem.* **1997**, *36*, 1541.
(28) (a) ADF 2.3.0. Theoretical Chemistry, Vrije Universiteit, Amsterdam. (b) Baerends, E. J.; Ellis, D. E.; Ros, P. *Chem. Phys.* **1973**, *2*, 41. (c) te Velde, G.; Baerends, E. J. *J. Comput.Phys.* **1992**, *99*, 84. (d) Fonseca Guerra, C.; Visser, O.; Snijders, J. G.; te Velde, G.; Baerends, E. J. In *Methods and Techniques for Computational Chemistry*; Clementi, E., Corongiu, G., Eds.; STEFF: Cagliari, Italy, 1995; p 305.
(29) (a) Snijders, J. G.; Baerends, E. J.; Vernooijs, P. *At. Nucl. Data Tables* **1982**, *26*, 483. (b) Vernooijs, P.; Snijders, J. G.; Baerends, E. J. *Slater type basis functions for the whole periodic system*; Internal Report; Free University of Amsterdam: Amsterdam, 1981.
(30) Vosko, S. J.; Wilk L.; Nusair, M. *Can. J. Phys.* **1980**, *58*, 1200.
(31) Versluis, L.; Ziegler, T. *J. Chem. Phys.* **1988**, *88*, 322.
(32) Ziegler, T.; Tschinke, V.; Baerends, E. J.; Snijders, J. G.; Ravenek, W. *J. Phys. Chem.* **1989**, *93*, 3050.
(33) Becke, A. D. *Phys. Rev. A.* **1988**, *38*, 3098.
(34) Perdew, J. P. *Phys. Rev. B.* **1986**, *33*, 8822.
(35) Schaftenaar, G. *MOLDEN*, Version 3.3; CAOS/CAMM Center Nijmegen: Toernooiveld, Nijmegen, The Netherlands, 1991.
(36) *ADFrom*, Version 1.2: Mariotti, F. Personal communication.
(37) Caulton, K. G. *New J. Chem.* **1994**, *18*, 25.

Table 1. Calculated Geometries (Å, deg) for $[W(CO)_5X]^-$ Species

X		W−X	W−C_{cis}	W−C_{trans}	C−O_{cis}	C−O_{trans}	X−M−C_{cis}
H		1.789	2.003	1.987	1.162	1.169	83.8
CH_3	in-plane	2.324 (2.313[a,b])	2.004 (1.999)	1.971 (1.975)	1.162 (1.179)	1.170 (1.164)	84.0 (87.8)
	out-of-plane		2.006		1.162		86.0
NH_2	in-plane	2.217	2.018	1.968	1.161	1.173	89.7
	out-of-plane		2.008		1.162		89.3
OH	in-plane	2.141 (2.192[c])	2.009 (2.009)	1.967 (1.875)	1.161 (1.161)	1.174 (1.229)	90.1 (93.2)
	out-of-plane		2.015		1.160		90.2
F		2.052	2.016	1.972	1.161	1.174	91.1
Cl		2.540	2.010	1.940	1.158	1.172	89.3
Br		2.679	2.011	1.944	1.157	1.171	87.8
I		2.898 (2.871[b,d])	2.013 (2.06)	1.944 (1.97)	1.157 (1.09)	1.171 (1.14)	87.6 (89.2)

[a] Darensbourg, D. J.; Bauch, C. G.; Rheingold, A. L. *Inorg. Chem*. **1987**, *26*, 977. [b] The average of the experimentally determined values is given. [c] Data are for $[Et_4N][W(CO)_5OPh]$ and are average values from the two independent molecules present in the unit cell. Darensbourg, D. J.; Sanchez, K. M.; Reibenspies, J. H.; Rheingold, A. L. *J. Am. Chem. Soc.* **1989**, *111*, 7094. [d] Palitzsch, W.; Böhme, U.; Roewer, G. *J. Chem. Soc., Chem. Commun*. **1997**, 803.

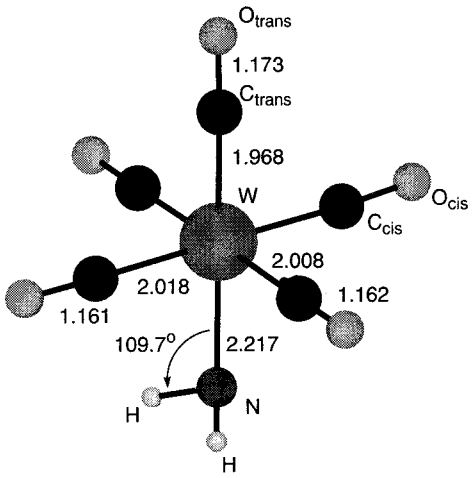

Figure 1. Calculated structure (Å, deg) of $[W(CO)_5NH_2]^-$.

various combinations of the 5σ and 1π CO orbitals. Of these, the $1a_2$ orbital is entirely CO 1π in character and nonbonding by symmetry with all of the metal-based orbitals. The $10a_1$ and $4b_1$ orbitals both display significant metal character and are W−CO σ-bonding.

The LUMO of $[W(CO)_5H]^-$ (11e) is mainly CO $2\pi^*$ in character, and to higher energy lie a further number of CO-based orbitals. Normally the metal−ligand σ-antibonding orbitals (e_g of the octahedron) might be expected to be among the lowest-lying unoccupied orbitals, but the first metal-based orbital ($13a_1$) is exclusively W 6s in character. The e_g-type orbitals are in fact $7b_1$ and $14a_1$ and lie more than 7 eV above the HOMO. This is much larger than the equivalent gap reported for $Mn(CO)_5Cl$ (3.5 eV)[38] but is a common feature of all the $[M(CO)_5X]^-$ species discussed here. Frontier orbital energies and compositions for $[W(CO)_5H]^-$ are provided as Supporting Information.

Although formally of lower symmetry, the frontier orbitals of $[W(CO)_5CH_3]^-$ are very similar to those of $[W(CO)_5H]^-$, suggesting that the methyl ligand is behaving essentially as a σ-donor ligand. Substitution with halides, however, results in M−X π-antibonding in the HOMO ($d\pi^*$) and the formation of an M−X π-bonding combination ($d\pi$). The $3b_2$ orbital has δ symmetry with respect to the M−X bond and is virtually unchanged by the introduction of π-donors. The energies of these orbitals (and their equivalents for the C_s structures; see below) are compared in Figure 2, where the $1a_2$ orbital has been used to provide a reference energy in each case.[39] The energy of the HOMO should reflect the strength of π-donation from X, and this orbital is indeed most stable in the absence of π-donation (X = H, CH_3), while for the halo pentacarbonyls it is most destabilized when X = F. In $[W(CO)_5NH_2]^-$ and $[W(CO)_5OH]^-$, the degeneracy of the $d\pi^*$ HOMO is removed to give the 15a″ and 28a′ orbitals. The energies of these orbitals indicate that π-donation is strong in the 15a″ (X = OH) and 28a′ (X = NH_2) HOMOs of these species but rather weak in their 28a′ (X = OH) and 15a″ (X = NH_2) partners.

The composition of the $d\pi^*$ orbitals of $[W(CO)_5X]^-$ species is given in Table 2a. M−X π-interaction causes a reduction in the metal d-character relative to the HOMO of $[W(CO)_5H]^-$. With π-donors, metal d-character is greatest when X = F and decreases along the series X = F to I and from X = F to NH_2. These trends follow the electronegativity of the donor atoms, with more efficient M−X mixing occurring when X has high-lying donor orbitals. Reduced metal character also results in a smaller CO $2\pi^*$ contribution, especially for the cis ligands.

For $[W(CO)_5NH_2]^-$ and $[W(CO)_5OH]^-$, the energies of the 15a″ and 28a′ orbitals reflect the very different π-donor capacities of these ligands in and out of the plane of symmetry. The X ligand contribution in the HOMOs of these systems (28a′, X = NH_2; 15a″, X = OH) is almost completely 2p in character and results in strong π-destabilization. π-Interaction is much reduced in the 28a′ orbital of $[W(CO)_5OH]^-$ and is virtually nonexistent in the 15a" orbital of $[W(CO)_5NH_2]^-$. In the latter, the out-of-plane N 2p orbital is mainly involved in N−H bonding (cf. the b_2 orbital of the free C_{2v} amide ligand) and is too low in energy for efficient π-interaction with the metal center.

The introduction of π-donors also results in a degree of cis M−CO σ-antibonding character mixing into the $d\pi^*$ orbitals. For $[W(CO)_5F]^-$, 1.2% W 6p character mixes with 2.1% CO 5σ, while the HOMO of $[W(CO)_5H]^-$ has less than 0.2% CO 5σ character. The differences are small, but the influence of this σ-antibonding character can be seen in the orbital representations and schematically in Figure 3. For $[W(CO)_5H]^-$, strong M−CO π-interaction occurs for both the cis and trans carbonyl ligands. Strong π-interaction is retained for the trans

(38) The study on $Mn(CO)_5Cl$ included gradient corrections self-consistently in the calculations of geometries and energies. However, using this same method, the calculated HOMO − "e_g" gap in $[W(CO)_5H]^-$ is still significantly larger at 7.1 eV.

(39) In the C_s structures (X = CH_3, NH_2, OH), some mixing of this orbital (now a″) with orbitals of like symmetry may occur, but an orbital retaining essentially a_2 character and having no metal contribution can be located in the electronic structure of these species and was used as the reference energy in each case.

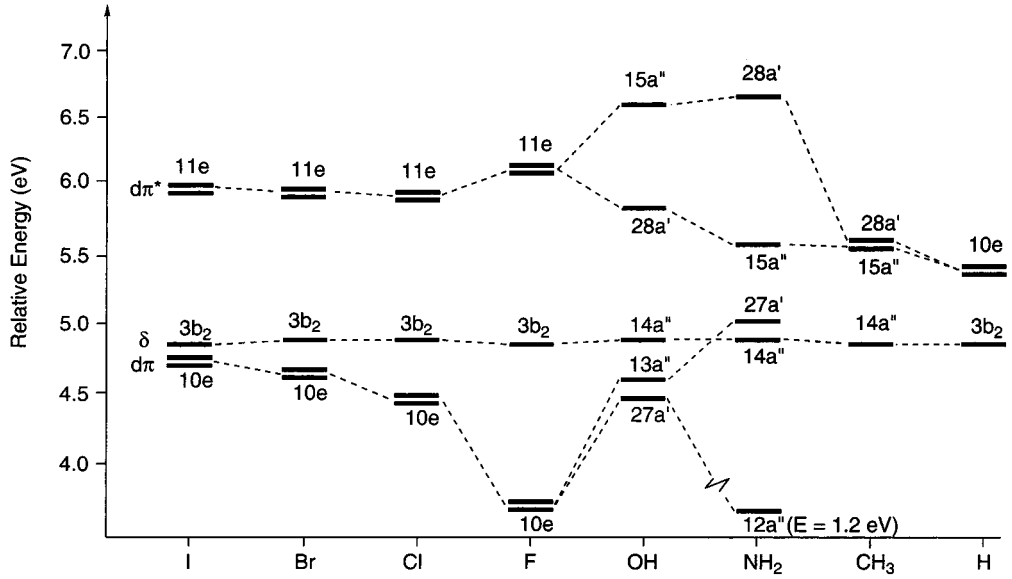

Figure 2. Relative energies (eV) of dπ*, δ, and dπ orbitals of $[W(CO)_5X]^-$ species.

Table 2

(a) Percentage Compositions for dπ* Orbitals of $[W(CO)_5X]^-$ Species

	%					
X	W p	W d	CO_{trans} 2π*	CO_{cis} 5σ	CO_{cis} 2π*	X
H	1.5	51.7	15.6	0.2	26.4	0.0
CH_3	1.3	50.7	15.7	0.0	24.6	3.3
NH_2 (28a′)	2.2	14.3	11.0	1.8	9.7	56.8
OH (15a″)	2.4	18.9	13.3	2.3	13.4	48.4
F	1.2	33.2	15.0	2.1	22.3	23.7
Cl	1.4	29.8	12.7	1.2	14.3	38.2
Br	1.4	27.2	11.5	0.7	11.5	45.8
I	1.1	20.6	9.2	0.6	7.6	59.6
NH_2 (15a″)	0.5	51.0	14.5	0.4	26.1	2.5
OH (28a′)	0.8	40.6	14.0	1.1	22.8	16.1

(b) Percentage Compositions for dπ Orbitals of $[W(CO)_5X]^-$ Species

	%					
X	W p	W d	CO_{trans} 2π*	CO_{cis} 5σ	CO_{cis} 2π*	X
NH_2 (27a′)	0.0	34.7	6.3	0.0	16.6	33.4
OH (13a″)	0.1	32.3	4.4	0.3	13.1	45.0
F	0.3	18.1	1.4	1.2	5.3	70.3
Cl	0.1	23.7	3.5	0.7	10.3	58.1
Br	0.0	26.9	4.5	0.9	12.6	50.8
I	0.0	34.9	6.5	0.8	15.7	37.1
NH_2 (12a″)	0.0	1.8	0.0[a]	2.3	14.6	45.4
OH (27a′)	2.3	10.5	1.1	0.1	5.2	70.2

[a] This orbital contains a 35.2% contribution from the CO_{trans} 1π orbital.

M−CO bond in $[W(CO)_5F]^-$ but is reduced via mixing-in of M−CO σ-antibonding character in the cis M−CO bonds.

The extent of this σ-antibonding effect generally follows the strength of π-donation from X. Thus, for $[W(CO)_5NH_2]^-$ (Figure 4), cis M−CO π-back-donation is disrupted in the 28a′ orbital but is relatively unaffected in the 15a″ orbital. The similarity of the latter with the HOMO of $[W(CO)_5H]^-$ suggests that the amide ligand is effectively a σ-donor in its out-of-plane interaction with the metal center.

Table 2b gives the composition of the dπ orbitals of $[W(CO)_5X]^-$ species. Considering only the plane of strong π-donation for the OH and NH_2 ligands, trends in metal and CO 2π* character again follow donor atom electronegativities and complement the trends highlighted for the equivalent dπ* orbitals. The equivalent "dπ" orbitals in the plane of weak

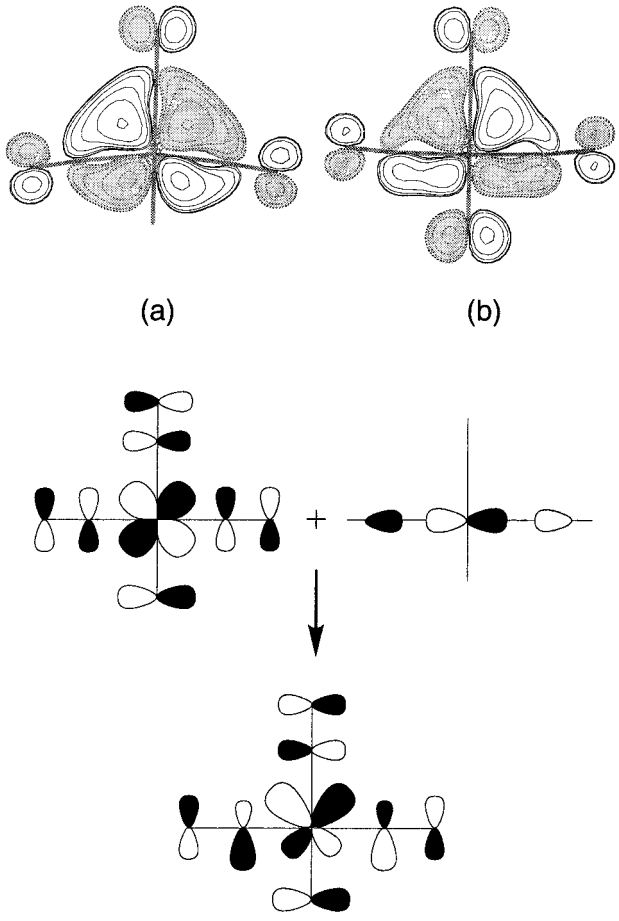

Figure 3. Orbital plots for dπ* HOMOs of (a) $[W(CO)_5H]^-$ and (b) $[W(CO)_5F]^-$ and a schematic representation of the effect of the mixing-in of M−CO σ-antibonding character.

π-donation are the 12a″ (X = NH_2) and 27a′ (X = OH) orbitals. These orbitals differ from the other dπ orbitals in that, although they are heavily localized on the X ligands, they contain little metal character. The major amide contribution to the 12a″ orbital of $[W(CO)_5NH_2]^-$ is the b_2-type N−H bonding orbital discussed above.

3. CO Dissociation. In common with earlier studies on $Mn(CO)_5X$ species,[25,26] we have divided the CO dissociation

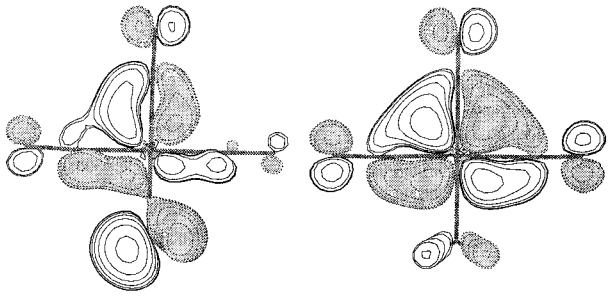

Figure 4. Orbital plots for 28a′ and 15a″ of $[W(CO)_5NH_2]^-$.

Table 3. M−CO Interaction Energies (kcal/mol) for $[M(CO)_5X]^-$ Species

		M = Cr		M = Mo		M = W	
X		cis	trans	cis	trans	cis	trans
H		52.1	61.0	48.3	53.6	54.9	61.4
CH_3	in-plane	47.7	63.2	45.1	56.4	51.7	64.5
	out-of-plane	48.3		45.5		51.6	
NH_2	in-plane	35.7	65.2	33.9	59.7	38.3	68.1
	out-of-plane	45.5		43.2		49.4	
OH	in-plane	38.2	65.9	37.3	61.6	45.3	70.9
	out-of-plane	32.3		32.5		37.6	
F		33.1	65.9	35.5	63.9	41.4	73.0
Cl		39.8	65.8	37.1	64.0	42.8	73.6
Br		39.4	65.2	38.0	63.7	44.0	73.5
I		41.1	64.9	38.9	63.3	45.5	73.6

process into two steps. Ground-state effects will be assessed by calculating the M−CO interaction energy—the energy required to remove a CO ligand from the 18e $[M(CO)_5X]^-$ species to produce the T_{CO} or T_X complex fragments. Relaxation energies in the 16e $[M(CO)_4X]^-$ species will be calculated by optimizing the geometries of the complex fragments in C_s symmetry. The CO dissociation energy is the sum of these two terms. We have also investigated the course of the CO dissociation processes by computing reaction profiles for cis and trans CO loss from $[W(CO)_5H]^-$ and $[W(CO)_5NH_2]^-$.

Metal−Carbonyl Interaction Energies in $[M(CO)_5X]^-$ Species. Computed cis and trans M−CO interaction energies are given in Table 3. For X = CH_3, NH_2, and OH, two values for the cis CO data are given, one corresponding to loss of a CO ligand from an out-of-plane position and the other being the lower of the values calculated for the two in-plane CO ligands. The data given in Table 3 (and the CO dissociation energies in Table 6) do not include a correction for basis set superposition error (BSSE). However, BSSE calculations (counterpoise method[40]) for $[W(CO)_5X]^-$ species consistently gave values around 2.5 kcal/mol and the total variation across the series was less than 1 kcal/mol, insufficient to change any of the trends discussed below.

For a given X, M−CO interaction energies generally follow the trend W > Cr > Mo. The only exceptions are for the cis M−CO bonds of $[Cr(CO)_5F]^-$ and $[Cr(CO)_5OH]^-$, which are slightly weaker than their Mo congeners. Interaction energies for trans M−CO bonds are always greater than those for cis M−CO bonds, and the difference between the two is significantly larger when X is a π-donor. For the amido species, in-plane cis M−CO interaction energies are about 10 kcal/mol lower than the out-of-plane values, while in the hydroxo analogues out-of-plane cis M−CO interaction energies are about 6 kcal/mol lower. Cis M−CO interaction energies are strongly dependent on X and, considering only the lowest values for the C_s species, follow the trends X = H > CH_3 > I > Br > Cl > F > NH_2 > OH for M = W and Mo and X = H > CH_3 > I > Cl > Br > NH_2 > F > OH for M = Cr. The reasons for the slightly different ordering when M = Cr are not clear to us at this time. In contrast, trans M−CO interaction energies are lowest when X is a σ-donor (H or CH_3) but show relatively little variation when X is a π-donor. The presence of a π-donor therefore results in a significantly stronger trans M−CO interaction but, contrary to arguments based on simple π-bonding, a weakened cis M−CO interaction. This weakening is greatest for the "hard" fluoride, hydroxide, and amide donor ligands.

(40) Boys, S. F.; Bernardi, F. *Mol. Phys.* **1970**, *19*, 553.

Table 4. Calculated Geometries (Å, deg) for Y_X $[W(CO)_4X]^-$ Species

X	W−X	W−C_{ax}	W−C_{eq}[a]	C−O_{ax}	C−O_{eq}[a]	α
H	1.800	1.996	1.926	1.166	1.177	88.7
CH_3	2.163	1.995	1.937	1.167	1.176	89.5
NH_2	2.015	1.999	1.946	1.168	1.176	90.7
OH	2.002	2.003	1.934	1.168	1.176	88.0
F	1.969	2.002	1.929	1.165	1.177	85.0
Cl	2.400	2.009	1.918	1.164	1.175	89.0
Br	2.546	2.003	1.915	1.163	1.175	89.0
I	2.779	2.002	1.912	1.162	1.174	87.7

[a] Geometries were optimized in C_s symmetry, and average values for these parameters are given.

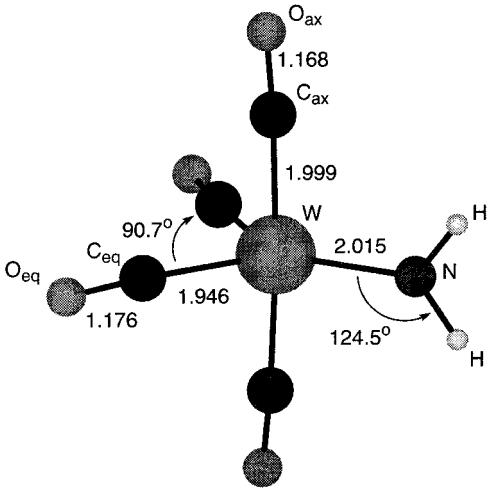

Figure 5. Calculated structure (Å, deg) of Y_X $[W(CO)_4NH_2]^-$.

Relaxation Energies in $[M(CO)_4X]^-$ Species. When X is a π-donor, optimization of the square-pyramidal T_{CO} complex fragments results in significant stabilization to give a Y_X geometry close to the archetypal bent C_{2v} shape. Y_X geometries were also computed when X = CH_3 (M = Cr, Mo, W) and X = H (M = Mo, W). $[Cr(CO)_4H]^-$ retains a T_{CO} structure. Calculated geometries for Y_X $[W(CO)_4X]^-$ species are given in Table 4, and the structure of $[W(CO)_4NH_2]^-$ is shown in Figure 5, along with the labeling scheme employed. With π-donors, relaxation energies (Table 5) follow the trend X = NH_2 > OH > F > Cl > Br > I, while a general increase is computed down the triad. The NH_2 and OH ligands are oriented so that the stronger π-donor orbitals of these ligands interact with the π-acceptor orbital of the $\{M(CO)_4\}$ fragment. That such π-donation is favorable is shown by the trigonal-planar geometry adopted by the amido ligand (cf. the pyramidal geometry of this moiety in 18e $[M(CO)_5NH_2]^-$). M−X distances are also significantly shorter in Y_X $[M(CO)_4X]^-$ than in $[M(CO)_5X]^-$, the largest effect being computed when X = NH_2 (0.20 Å). This may again be a result of π-donation in the Y_X species, although a similar shortening is also computed when X = CH_3.

Table 5. Relaxation Energies (T_{CO} to Y_X; kcal/mol) for $[M(CO)_5X]^-$ Species[a]

X	M = Cr	M = Mo	M = W
H	3.9[b]	5.6	10.3
CH_3	7.5	9.6	14.2
NH_2	20.6	18.9	23.1
OH	15.7	15.2	19.1
F	12.8	13.4	17.4
Cl	11.8	10.4	14.2
Br	7.8	9.7	12.7
I	6.8	8.3	10.7

[a] For X = CH_3, NH_2, and OH, values correspond to the most stable T_{CO} structure. [b] Retains a T_{CO} structure upon optimization.

Table 6. CO Dissociation Energies (kcal/mol) for $[M(CO)_5X]^-$ Species

X	M = Cr	M = Mo	M = W
H	48.2	42.4	44.6
CH_3	40.2	35.5	37.4
NH_2	15.1	15.0	15.2
OH	16.7	17.4	18.6
F	20.4	22.1	23.9
Cl	28.0	26.7	28.7
Br	31.5	28.3	31.3
I	34.3	31.1	34.7

As was found for the 18e species, computed M−C and C−O bond lengths vary little as a function of X. $M-C_{ax}$ bonds are about 0.05−0.10 Å longer than $M-C_{eq}$ bonds, and $C-O_{ax}$ bonds are about 0.01 Å shorter than $C-O_{eq}$ bonds.

We have also considered relaxation of the T_X geometries for the tungsten species with optimizations performed in C_s symmetry. With the exception of $[W(CO)_4NH_2]^-$, a stationary point was located which was both geometrically and energetically close to the original T_X complex fragment. However, of these, only T_X $[W(CO)_4H]^-$ corresponded to an energy minimum (no negative frequencies), while, for X = CH_3, OH, or halide, a transition state had been located (one negative frequency). All attempts to optimize a stationary point corresponding to the T_X $[W(CO)_4NH_2]^-$ structure resulted in complete relaxation to the Y_X form.

The relative energies of the relaxed T_X and Y_X isomers are again a function of X. For $[W(CO)_4OH]^-$, T_X lies 49.2 kcal/mol higher in energy than Y_X, while, for $[W(CO)_4H]^-$, this difference is only 13.9 kcal/mol. In the cases where a relaxed T_X geometry could be located, it remained higher in energy than the unrelaxed T_{CO} complex fragment. This has implications for the fluxionality of Y_X species: First, structures based on a T_{CO} geometry are more likely to be involved in the exchange mechanism than those based on T_X structures. Second, assuming the intermediacy of T_{CO}-like structures, the $T_{CO} \rightarrow Y_X$ relaxation energies give a measure of the barrier for CO exchange, and this will be greatest when X = F, OH, or NH_2.

CO Dissociation Energies and Reaction Profiles for CO Loss. Loss of a cis CO ligand is computed to be more facile and, with the exception of $[Cr(CO)_4H]^-$, results in Y_X geometries. The computed CO dissociation energies presented in Table 6 therefore correspond to the energy difference between these Y_X species (plus free CO) and 18e $[M(CO)_5X]^-$. For all three metals, CO dissociation is always more facile when X is a π-donor and follows the trend X = NH_2 < OH < F < Cl < Br < I < CH_3 < H. Much less variation is computed down the triad, although generally CO dissociation is most facile from the Mo species. Upon trans CO loss, it is possible that the T_X structures may be involved as transition states (or, for X = H, an intermediate) along the pathway to give the more stable Y_X form. Likewise, although we have shown that the T_{CO} structures are not stable intermediates along the pathway for cis CO loss, the possibility that the transition state for this process might resemble this structure remains. To investigate these points we have computed reaction profiles for cis and trans CO loss from $[W(CO)_5H]^-$ and $[W(CO)_5NH_2]^-$. The reaction profile for cis CO loss was calculated in C_s symmetry, and we considered only the loss of the more weakly bound in-plane CO for $[W(CO)_5NH_2]^-$. For trans CO loss, the reaction profile was calculated in C_1 symmetry with the $W-CO_{trans}$ unit constrained to be linear throughout. For both systems, the lengthening of a cis W−CO bond was coupled to a smooth distortion of the T_{CO} $[W(CO)_4X]^-$ structure and the final Y_X form was effectively achieved at an M−C distance of 3.0 Å. A small activation barrier could be inferred from these reaction profiles but was less than 1 kcal/mol in both cases. In contrast, very little distortion of the T_X $[W(CO)_4X]^-$ fragment was found as the $W-CO_{trans}$ distance was increased. It seems likely therefore that dissociation of a trans CO ligand would entail passing through a transition state with a structure close to the T_X form and that no alternative low-energy pathway is available for loss of a trans CO ligand.[41]

Comparison with Neutral Analogues. (a) $M(CO)_6$. In a comparison of CO labilities for $[M(CO)_5X]^-$ species and their hexacarbonyl parents, the different overall charges of these species will clearly affect the bond dissociation energies. Two recent computational studies of CO dissociation from d^6 $M(CO)_6^n$ (M = Hf−Ir) species using density functional methods have found the first CO bond dissociation energy of $[Ta(CO)_6]^-$ to be greater than that of $W(CO)_6$ by about 2−3 kcal/mol.[42] This difference has been accredited to enhanced π-back-donation in the anionic species. Our computed CO dissociation energies for $M(CO)_6$ species (42.5, 38.2, and 44.8 kcal/mol for M = Cr, Mo, and W, respectively) are in good agreement with those calculated previously using similar methods.[42,43] As the $M(CO)_5$ fragments retain a T_{CO} structure, their relaxation energies are small and the major component of the dissociation energy arises from the M−CO interaction energies (43.3, 41.5, and 46.1 kcal/mol for M = Cr, Mo, and W, respectively). From a comparison with the data in Tables 3 and 6, it appears that the introduction of a π-donor both weakens the M−CO interaction energy and lowers the overall CO dissociation energies relative to those of $M(CO)_6$ species, as is seen experimentally.

(b) $M'(CO)_5X$ (M′ = Mn, Re) Species. Computed CO dissociation energies for $Mn(CO)_5X$ and $Re(CO)_5X$ species show a slight decrease relative to those of their anionic Cr and W analogues, in line with the $[Ta(CO)_6]^-/W(CO)_6$ comparison discussed above. All the group 7 18e species are computed to be thermodynamically stable with respect to CO loss: For M′ = Re, dissociation energies range from 9.4 (X = NH_2) to 48.3 kcal/mol (X = H). Trends in CO dissociation, M−CO interaction, and relaxation energies as a function of the X ligand are similar to those computed for the group 6 species.

Discussion

Experimentally, CO substitution reactions in $[M(CO)_5X]^-$ species are dissociative in nature and it has been shown that loss of a cis CO occurs more readily than loss of a trans CO

(41) This is consistent with the description of this process as "thermally disallowed". See ref 25.

(42) (a) Ehlers, A. W.; Ruiz-Morales, Y.; Baerends, E. J.; Ziegler, T. *Inorg. Chem*. **1997**, *36*, 5031. (b) Szilagyi, R.; Frenking, G. *Organometallics* **1997**, *16*, 4807.

(43) Li, J.; Schreckenbach, G.; Ziegler, T. *J. Am. Chem. Soc*. **1995**, *117*, 486.

ligand. The rate of reaction follows the order X = Cl > Br > I, while, qualitatively, $[W(CO)_5F]^-$ and $[W(CO)_5OH]^-$ appear even more labile than the heavier halide analogues. Our computed trends for CO dissociation energies are consistent with these findings. We would predict that the as yet unknown $[M(CO)_5NH_2]^-$ complexes would be the most labile of all the species studied here but remain viable targets for possible synthesis.

The calculations indicate that both ground-state and relaxation effects play a role in the variation in cis CO lability. For $[W(CO)_5X]^-$ species, computed cis M−CO interaction energies range from 54.9 (X = H) to 37.6 kcal/mol (X = OH). Variation in the relaxation energies is slightly less and spans 23.1 (X = NH_2) to 10.3 kcal/mol (X = H). Similar trends are seen in the computed data for the Cr and Mo analogues. Enhanced X → M π-donation has been identified as the driving force for the formation of the Y_X $[M(CO)_4X]^-$ intermediates.[25,26] Further support for this is found in the computed Y_X $[M(CO)_4OH]^-$ and $[M(CO)_4NH_2]^-$ structures, where the orientation of the X ligands maximizes π-donation to the metal center. Calculated relaxation energies can therefore provide a basis for ranking the π-donor capacity of the X ligands. Considering only the stronger π-donor phase of the NH_2 and OH ligands, our ordering would be X = NH_2 > OH > F > Cl > Br > I. This correlates reasonably well with both dπ* orbital energies in $[M(CO)_5X]^-$ species (Figure 2) and the general trends in computed cis M−CO interaction energies. Strong π-donation from X therefore weakens the cis M−CO interaction.

Computed reaction profiles for cis CO loss indicate that the T_{CO} complex fragment is not directly involved in the dissociation process either as an intermediate or as a transition-state species. M−CO interaction energies therefore do not give a direct measure of the ease of CO loss by approximating, for example, an activation energy. Rather, we interpret a low value for this parameter in terms of a general destablization of the ground-state $[M(CO)_5X]^-$ structure.[44] For X = F, OH, and NH_2, in particular, low cis M−CO interaction energies combine with large relaxation energies to produce low cis CO dissociation energies.

Variation in Cis M−CO Interaction Energies. The correlation between strong π-donation and reduced cis M−CO interaction energies is particularly clear in the $[M(CO)_5NH_2]^-$ and $[M(CO)_5OH]^-$ species. Of the systems featuring π-donors, these display both the lowest (X = NH_2, in-plane CO; X = OH, out-of-plane CO) and the highest values (X = NH_2, out-of-plane CO; X = OH, in-plane CO) for the cis M−CO interaction energies, and these trends are mirrored by the energies of the corresponding dπ* orbitals. Intermediate cis M−CO interaction energies and dπ* orbital energies are obtained when X is a halide, although the correlation between these two parameters within this group is not so strong. The cis M−CO interaction energies are strongest when X is a σ-donor such as H, CH_3, or, for the out-of-plane M−CO bond, the NH_2 ligand. Although the in- and out-of-plane cis M−CO interactions in $[M(CO)_5NH_2]^-$ species differ by about 10 kcal/mol, this is not reflected in the corresponding M−CO bond lengths, which are within 0.015 Å. Use of bond length as a criterion for bond strength may therefore be inappropriate for these species.

Further insight into the variation in cis M−CO interaction energies can be gained by considering the interaction of a CO ligand with the T_{CO} complex fragment. A schematic molecular orbital diagram for this process (Figure 6) shows the four major

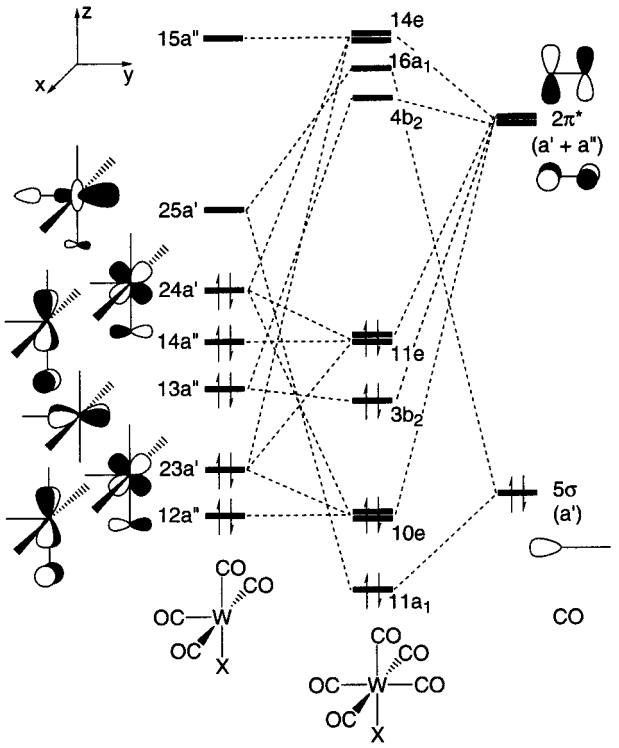

Figure 6. Schematic orbital correlation diagram for the interaction of a CO ligand with a T_{CO} complex fragment.

bonding interactions involved in cis M−CO bonding. σ-Donation from the CO 5σ lone pair to the 25a′ T_{CO} LUMO is reinforced by π-back-donation from the T_{CO} 13a″ and 24a′ orbitals into the 2π* orbital of CO. Further π-back-donation from the 23a′ orbital is also possible. The 14a″ and 12a″ T_{CO} fragment orbitals are nonbonding with respect to the cis CO. The nature of X can therefore influence cis M−CO bonding through participation in the 23a′, 24a′, and 25a′ T_{CO} orbitals (13a" exhibits no X-character). In the following, we shall focus on these orbitals, and while it is not possible to quantify how each M−CO interaction varies with the nature of X, indirect information can be obtained by considering their energy and degree of overlap with the appropriate CO orbital.[45]

The compositions of the 24a′ orbitals for the T_{CO} $[W(CO)_4X]^-$ fragments are given in Table 7. As π-donation from X becomes stronger the amount of computed metal d-character decreases while the p-character increases. This can be most clearly seen in the two T_{CO} $[W(CO)_4NH_2]^-$ fragments formed from in- and out-of-plane CO loss. The 24a′ orbital of the former displays 7.5% p- and 34.8% d-character, while the equivalent figures are 2.2% and 54.6% in the corresponding orbital of the latter. A possible driving force for this d/p mixing can be seen by considering a trans X−M−CO unit:

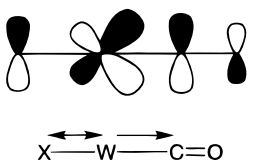

Hybridization of the electron density at the metal reduces Xπ−dπ 4e destabilization while enhancing π-back-donation to the

(44) Our results are closely related to Caulton's suggestion that filled/filled interactions in $W(CO)_5(OPR_3)$ species will destabilize the ground state. See ref 37.

(45) Orbital energies are relative to an a_2−type orbital (now minus one CO ligand, but still identifiable in the electronic structures of the T_{CO} fragments).

Table 7. Comparison of T_{CO} $[W(CO)_4X]^-$ 24a′ Orbital Compositions, Overlap Integrals with CO Fragment Orbitals, and cis M−CO Interaction Energies (kcal/mol)

		% metal character		overlap integrals		
X		d_{yz}	p_y	$\langle 24a'\|5\sigma\rangle$	$\langle 24a'\|2\pi^*\rangle$	interaction energy
H		59.5	0.8	0.02	0.22	54.9
CH_3		55.5	1.8	0.05	0.18	51.7
NH_2	in-plane	34.8	7.5	0.21	0.11	38.3
OH	out-of-plane[a]	36.4	7.7	0.21	0.12	37.6
F		42.6	5.9	0.19	0.14	41.4
Cl		45.7	3.7	0.14	0.14	42.8
Br		46.2	3.2	0.12	0.14	44.0
I		45.1	2.5	0.11	0.14	45.5
NH_2	out-of-plane[a]	54.6	2.2	0.11	0.21	49.4
OH	in-plane	47.4	4.0	0.15	0.14	45.3

[a] Data for metal contributions are for the p_x and d_{xz} orbitals.

$2\pi^*$ orbitals of the trans CO ligand. Strong π-donation from X increases the drive for this hydridization at the metal and results in greater metal p-character.

d/p mixing at the metal will also affect cis M−CO bonding, however. Computed overlap integrals (Table 7) show that stronger π-donation from X results in a general decrease in the overlap between the 24a′ orbital and the CO $2\pi^*$ orbital. In addition, with stronger π-donors, notably X = F, OH (out of plane), and NH_2 (in plane), an increase in the overlap with the CO 5σ orbital is also found. This will switch on M−CO σ-antibonding interactions of the type seen in the $d\pi^*$ HOMO of the 18e $[W(CO)_5X]^-$ species. As π-donation from X increases, cis M−CO bonding will be weakened due to both reduced M−CO π-back-donation and M−CO σ-antibonding effects.

The 25a′ LUMO of the T_{CO} fragment is slightly M−X π-antibonding in character and is therefore energetically most available when X is a simple σ-donor, becoming a poorer acceptor orbital as π-donation from X increases. The effect is small—this orbital is 0.25 eV more stable for X = H compared to X = I and is only 0.18 eV higher for X = NH_2, the strongest π-donor—but it is consistent with decreasing CO → M σ-donation (and weaker cis M−CO bonding) as the π-donor strength of X increases.

Trends in the energy and composition of the 23a′ M−X π-bonding orbital are similar to those described for the related $d\pi$ orbital of the 18e $[M(CO)_5X]^-$ species. High-lying donor orbitals on X raise both the energy and metal character of this orbital and should result in enhanced M−CO π-back-donation along the series from X = F to I, consistent with the computed variation in cis M−CO interaction energies. On this basis M−CO π-back-donation from 23a′ should also increase from X = F to NH_2, although this opposes the computed trend in cis M−CO interaction energy.

In summary, the major mechanism by which strong π-donors weaken cis M−CO bonding in $[M(CO)_5X]^-$ species is to induce d/p mixing at the metal center. This in turn disrupts M−CO π-back-donation and has the effect of switching on cis M−CO σ-antibonding interactions. Cis CO → M σ-donation is also diminished when X is a good π-donor. When X = F, OH, or NH_2, these factors combine to produce low cis M−CO interaction energies, indicative of a destabilization of the $[M(CO)_5X]^-$ species and contributing to the high CO lability of these species.

Trans Influence of X Donor Ligands. Computed trans M−CO interaction energies give a measure of the trans influence of the X donor ligands. As expected, the trans influence is highest (i.e., M−CO interaction energies are lowest) for the simple σ-donor hydride and methyl ligands. The lower trans influences obtained with the π-donor ligands are likely to result in part from enhanced M−CO π-back-donation. However, there does not seem to be a simple relationship between computed trans M−CO interaction energies and trends in π-donor strength. It is likely that σ-donor effects will also be important in determining the trans influence of X, and an assessment of the relative importance of σ- and π-donation in determining M−X bond strengths is the subject of ongoing work in our group.[46]

Conclusion

We have investigated CO lability in a series of $[M(CO)_5X]^-$ species (M = Cr, Mo, W) using density functional methods. For all three metals, CO dissociation energies follow the trend X = NH_2 < OH < F < Cl < Br < I < CH_3 < H, and this ordering is consistent with the available experimental data. In agreement with earlier studies, we have found that CO dissociation is promoted by π-stabilization of the 16e species formed. We have demonstrated that the ability of the π-donors to act in this way is greatest for X = NH_2 > OH > F > Cl > Br > I. However, for X = NH_2 and OH, π-donor ability depends on the orientation of the ligand. In addition, we have shown that π-destabilization of the ground-state 18-e species is equally significant in promoting CO lability. This can be traced to a hybridization of the electron density at the metal, the extent of which depends on the degree of π-donation from X. The metal rehybridization enhances trans M−CO π-back-donation, but it both reduces cis M−CO π-back-donation and induces cis M−CO σ-antibonding interactions, which serve to weaken the cis M−CO bond.

Acknowledgment. We thank the EPSRC for funding through the "Fast Track" Scheme, The Royal Society for an equipment grant, and Heriot-Watt University for support.

Supporting Information Available: Listings of computed Cartesian coordinates for all $[M(CO)_5X]^-$ and Y_X $[M(CO)_4X]^-$ species and frontier orbital energies and compositions for $[W(CO)_5H]^-$. This material is available free of charge via the Internet at http://pubs.acs.org.

IC990355N

(46) Macgregor, S. A.; MacQueen, D. Work in progress.